Frontiers in Bioscience Landmark

Front. Biosci. (Landmark Ed) **2025**; 30(4): 37430
https://doi.org/10.31083/FBL37430

Original Research

Macrophage Notch1 Participates in LPS-Induced Acute Lung Injury via Regulating CCR5 Expression in Mice

Ruiyu Zhang[1,†], Hui Du[1,†], Zhi Liu[1], Yuxi Lei[1], Huizhi Hu[1], Junwen Zheng[1], Pu Yang[1,2,*], Dongchi Zhao[1,2,*]

[1]Department of Pediatrics, Zhongnan Hospital of Wuhan University, 430071 Wuhan, Hubei, China
[2]Children's Digital Health and Data Center of Wuhan University, 430071 Wuhan, Hubei, China
*Correspondence: puer58@hotmail.com (Pu Yang); zhao_wh2004@hotmail.com (Dongchi Zhao)
[†]These authors contributed equally.

Academic Editors: Esteban C. Gabazza and Srinivasa Reddy Bonam
Submitted: 27 January 2025 Revised: 22 March 2025 Accepted: 27 March 2025 Published: 23 April 2025

Abstract

Background: As pivotal immunoregulatory sentinels in pulmonary defense systems, alveolar macrophages (AMs) play dual roles in mediating inflammatory responses and tissue repair processes during various phases of inflammatory cascades. The present investigation focuses on elucidating the regulatory influence of Notch pathway activation within AM populations on the pathophysiological mechanisms underlying acute lung injury (ALI) development. **Methods**: To investigate the regulatory roles of Notch intracellular domain (NICD) and C-C chemokine receptor type 5 (CCR5) in pulmonary inflammation, an ALI model was established through lipopolysaccharide (LPS) administration. Complementary studies used macrophage-specific Notch1 knockout mice and immortalized bone marrow-derived macrophages (iBMDMs). Molecular profiling of CCR5 and inflammatory mediators was performed through real-time quantitative reverse transcription PCR (qRT-PCR) and immunofluorescence staining. Functional assessments of macrophage migration were carried out using scratch wound healing assays and transwell migration assays. **Results**: In the LPS-induced ALI model, pulmonary tissues exhibited elevated expression of both NICD and CCR5. Conversely, Notch1 knockout mice attenuated CCR5 expression, reduced macrophage infiltration and downregulated transcription of pro-inflammatory mediators compared to wild-type controls ($p < 0.05$). Lung injury was milder in the Notch1-deficient mice model compared to wild mice ($p < 0.05$). *In vitro* experiments demonstrated that inhibiting the Notch pathway in macrophages reduced CCR5 expression and attenuated CCL5-induced macrophage migration. **Conclusion**: Notch signaling regulates macrophage infiltration and the inflammatory response by modulating CCR5 expression in ALI induced by LPS.

Keywords: acute lung injury; alveolar macrophages; Notch; CCR5; cell migration

1. Introduction

Acute lung injury (ALI) is a severe inflammatory lung disease, characterized by hypoxemia and progressive respiratory distress, which may progress to acute respiratory distress syndrome (ARDS) in clinically severe presentations [1]. The activation of alveolar macrophage (AMs) leading to excessive inflammatory responses is a primary cause of damage to alveolar cells, which results in heightened alveolar-capillary permeability, fibrin exudation into the alveoli, diffuse interstitial edema, reduced lung compliance, ultimately, impairment of pulmonary gas exchange [2].

The excessive activation of inflammation caused by infection is one of the key pathological foundations of ALI. AMs play a crucial role in recognizing and phagocytosing pathogens and necrotic cells while also maintaining the balance of the local microenvironment [3]. During the acute phase of inflammation, activated AMs undergo phenotypic polarization, accompanied by significant functional alterations. These polarized macrophages recruit additional inflammatory cells to migrate to the lungs and release a variety of inflammatory mediators, thereby amplifying the inflammatory response. Macrophage polarization can be initiated through the recognition of inflammatory cells or stimulation by cytokines, with the Notch signaling pathway playing a pivotal role in this process. This pathway regulates macrophage polarization by binding to its ligands (Jagged/Delta) and subsequently initiating nuclear transcription [4]. In addition to cytokine release, polarized AMs also participate in intercellular signaling through Notch receptors, altering their immune phenotype and exerting both pro-inflammatory and anti-inflammatory effects at different stages [5,6]. Therefore, Notch deficiency can lead to incomplete immune responses.

C-C chemokine receptor type 5 (CCR5) is a receptor for β-chemokines (such as CCL3, CCL4, and CCL5). This G protein-coupled receptor exhibits predominant surface expression on quiescent T lymphocytes, neutrophils, circulating monocytes, and dendritic cells. CCR5-mediated signaling orchestrates can modulate the recruitment and functional activation of mononuclear phagocytes. CCR5 is an important co-receptor for the entry of human immunodeficiency virus type 1 (HIV-1) and is widely involved in the pathogenesis of various diseases [7]. Transcrip-

tomic analysis revealed that the levels of CCL3, CCL4, and CCR5 were significantly elevated in the lung tissues of ALI mouse models, suggesting that CCR5 may act as a key regulator of the inflammatory response by coordinating chemokine-mediated immune cell infiltration [8]. Notably, pharmacological blockade of the CCL3/CCR5 axis significantly reduced monocyte chemotaxis in response to sputum supernatants from chronic obstructive pulmonary disease patients, further highlighting the role of this pathway in sustaining leukocyte recruitment during chronic inflammatory lung diseases [9]. Accumulating evidences indicate that pharmacological inhibition of CCR5-mediated signaling pathways may effectively mitigate excessive immune activation and cytokine storm syndrome associated with severe COVID-19 manifestations, and reduce neutrophil and monocyte accumulation, as well as diffuse alveolar damage in lung injury models [10,11]. Research indicates that the coordinated activation of CCR5 receptor signaling and the Notch signaling pathway plays a crucial role in the pathogenesis and immune regulation of autoimmune encephalitis [12]. However, the mechanisms by which Notch polarization affects CCR5 chemotactic activity promotes inflammatory cell aggregation, and exacerbates lung injury remain unclear.

This study investigated the regulatory relationship between macrophage Notch1 signaling and CCR5 expression dynamics in the ALI murine model. The results showed that macrophage Notch1 signaling deficiency reduced CCR5 expression, inhibited cell migration, and suppressed the release of inflammatory mediators, thereby exerting lung-protective properties against ALI progression in experimental mice.

2. Methods

2.1 Animals and ALI Models

Myeloid-specific Notch1 knockout mice (C57BL/6J background) were generated by targeted gene deletion, and the knockout mice ($Notch1^{cre+}$) and wild-type control mice ($Notch1^{flox+}$) were produced by Cyagen Biotechnology (Suzhou, China) and referred to as Cre and Flox mice respectively. Male mice (4–6 weeks old, 14–18 g) were selected for the experiments. The experimental mice were maintained under specific pathogen-free (SPF) conditions, with temperature regulated at 22 ± 1 °C and relative humidity maintained at 60%. All animal care and experimental protocols were approved by the Animal Ethics Committee of Wuhan University (Wuhan, China, Project No. WP20240088).

The ALI models were established following previously described methods [13]. $Notch1^{flox}$ mice were divided into three experimental groups (n = 5 per group): the control group (saline), the lipopolysaccharide (LPS) group (LPS), and the LPS+Mvc group (LPS + Maraviroc). Specifically, mice were anesthetized with sodium pentobarbital (1%, 70 mg/kg, i.p.) and then administered LPS via tracheal injection. $Notch1^{cre+}$ mice were randomly assigned to two groups (n = 5 per group): the saline control group and the LPS group. For the ALI model, mice were given 3 mg/kg LPS (S1732, Beyotime, Shanghai, China) via intratracheal injection. A dose of 10 µg/g Maraviroc (CCR5 antagonist, HY-13004, MedChemExpress, Monmouth County, NJ, USA) was administered 30 minutes prior to LPS induction. After 24 hours, all mice were humanely euthanized by CO_2 asphyxiation (20% chamber volume per minute) to minimize suffering, followed by cervical dislocation as a secondary confirmatory method. Peripheral blood was collected via retro-orbital venous plexus puncture. The thoracic cavity was rapidly accessed through a midline sternotomy, and bilateral lung tissues were resected en bloc. The harvested specimens were used for subsequent histopathological evaluation, real-time quantitative reverse transcription PCR (qRT-PCR), and western blotting analysis.

2.2 Histopathological Evaluation

Post-fixation, lung tissue specimens underwent sequential ethanol dehydration followed by paraffin embedding to generate histological sections. After the Hematoxylin and eosin (G1120, Solarbio, Beijing, China) staining of lung tissue sections, the slides were observed under an optical microscope (Leica, Wetzlar, Germany) for histopathological examination and quantitative lung injury scoring [14]. For each tissue slide, five different areas were selected and examined at high magnification (200×).

2.3 Lung Wet/Dry (W/D) Ratio

Fresh lung tissue was carefully blotted with absorbent paper to remove surface moisture and blood, and its wet weight was recorded. Then, the samples were incubated in a 60 °C constant-temperature incubator for 72 hours. Following complete desiccation, the tissue mass was recorded. The gravimetric ratio was determined to assess pulmonary edema severity.

2.4 Extraction of Bronchoalveolar Lavage Fluid (BALF)

500 µL of chilled phosphate-buffered saline (PBS) was injected through intratracheal instillation and gently aspirated to obtain BALF. This lavage procedure was iterated three times to maximize fluid recovery. The pooled BALF was subjected to centrifugation and the supernatant was aliquoted for protein quantification. The remaining cellular fraction was washed twice with PBS before resuspension for quantitative analysis.

2.5 Cell Culture

Immortalized bone marrow-derived macrophages (iBMDMs) were purchased from Cyagen Bioscience Inc., Guangzhou, China. We validated all cell lines by Short Tandem Repeat (STR) profiling. All cells were confirmed to be mycoplasma-free by testing with a PCR-based mycoplasma

Table 1. Sequences of primers for qRT-PCR.

Gene	Sense (5′-3′)	Anti-sense (3′-5′)
CCR5	ATGGATTTTCAAGGGTCAGTTCC	CTGAGCCGCAATTTGTTTCAC
TNF-α	GGCTGCCCCGACTACGT	AGGTTGACTTTCTCCTGGTATGAGA
IL-6	CCGGAGAGGAGACTTCACAG	ACAGTGCATCATCGCTGTTC
IL-1β	TCATTGTGGCTGTGGAGAAG	AGGCCACAGGTATTTTGTCG
GAPDH	AGGTCGGTGTGAACGGATTTG	GGGGTCGTTGATGGCAACA

qRT-PCR, real-time quantitative reverse transcription PCR; *CCR5*, C-C chemokine receptor type 5; *TNF-α*, tumour necrosis factor-alpha; *IL*, interleukin; *GAPDH*, Glyceraldehyde-3-phosphate dehydrogenase.

detection kit (C0301S, Beyotime, Shanghai, China), ensuring the absence of contamination. The iBMDM cell line was maintained in high-glucose DMEM containing 10% FBS (Gibco, Carlsbad, CA, USA) under standard culture conditions (37 °C, 5% CO_2). For experimental treatments, cells were pre-incubated with MK-0752 (γ-secretase inhibitor, HY-10974; MedChemexpress, Monmouth County, NJ, USA) for 24 hours prior to LPS (1 µg/mL) challenge.

2.6 Western Blot

After protein extraction, samples were subjected to sodium dodecyl sulfate-polyacrylamide gel electrophoresis (SDS-PAGE) for molecular separation. Subsequently, the resolved proteins were electrophoretically transferred onto polyvinylidene fluoride (PVDF) membranes, which were then incubated with 5% non-fat dry milk for 60 minutes at ambient temperature to prevent non-specific binding. Primary antibodies were applied according to the experimental requirements and incubated overnight at 4 °C: CCR5 (BS77962, 1:1000, Bioworld Biotechnology, Nanjing, China), NICD detection using Cleaved Notch1 (V1744) antibody (4147S, 1:1000, Cell Signaling Technology, Danvers, MA, USA), GAPDH (GB15004, 1:6000, Servicebio Biotech, Wuhan, China). After washing with Tris-Buffered Saline with Tween 20 (TBST), the membrane was incubated with the secondary antibody, Goat Anti-Rabbit IgG (H+L) HRP (A0208, 1:1000, Beyotime, Shanghai, China) at room temperature for 1 hour, followed by washing with TBST. Protein bands were visualized using Enhanced Chemiluminescence (ECL) (A10016, Abmart, Shanghai, China) detection. The quantification of blots was performed by using ImageJ software (version 1.8.0, NIH, Bethesda, MD, USA).

2.7 Real-time Quantitative Reverse Transcription PCR (qRT-PCR)

Total RNA isolation from pulmonary tissues and cultured cells was carried out with Trizol reagent (15596026, Thermo Fisher Scientific, Waltham, MA, USA). RNA integrity and concentration were assessed spectrophotometrically using a Nanodrop One instrument (Thermo Fisher Scientific). Subsequently, cDNA was synthesized by reverse transcription. Quantitative real-time PCR analysis was conducted with 2×Universal Blue SYBR Green qPCR Master Mix (G3326, Servicebio Biotech, Wuhan, China) in triplicate technical replicates per sample. Relative mRNA expression levels were determined through the comparative $\Delta\Delta$Ct method. Primer sequences are listed in Table 1.

2.8 Flow Cytometry

Fresh lung tissue was prepared for flow cytometry analysis. 1× red blood cell lysis buffer was added into the cell suspension, after a standing time of 3 minutes, the mixture was then centrifuged. The cells were then resuspended in 100 µL PBS and blocked with 2 µL of anti-mouse CD16/CD32 (65080-1-Ig, 0.5 mg/mL, Proteintech Group, Wuhan, China) antibody at 4 °C for 10 minutes. The cells were stained with fluorescently conjugated antibodies: APC-A750 anti-mouse CD45 antibody (E-AB-F1136, 5 µL/mL, Elabscience, Wuhan, China) and PE-A anti-mouse CD64 antibody (E-AB-F1186, 5 µL/mL, Elabscience, Wuhan, China) for 60 minutes in the dark at 4 °C. After washing, the samples were analyzed by flow cytometer (Beckman Coulter, Brea, CA, USA).

2.9 Enzyme-linked Immunosorbent Assay (ELISA)

Enzyme Following the manufacturer's protocols, the ELISA kits (Nanjing Jiancheng Bioengineering Institute, Nanjing, China) were used to measure the concentrations of interleukin (IL)-6 (H007-1), IL-1β (H002-1), and tumour necrosis factor-alpha (TNF-α) (H052-1) in mouse serum.

2.10 Immunofluorescence Staining

Lung tissue sections embedded in paraffin were subjected to deparaffinization and rehydration processes. Antigen retrieval was achieved through microwave-mediated heating. Primary antibody incubation was performed overnight at 4 °C using anti-CCR5 (1:50 dilution, BS77962, Bioworld Biotechnology, Nanjing, China) and anti-F4/80 (1:200 dilution, ab6640; Abcam, Cambridge, UK). Following three washes with PBS, samples were exposed to species-specific secondary antibodies: AF488-labeled Goat Anti-Rabbit IgG (H+L) (1:300 dilution, A0423, Beyotime, Shanghai, China), Cy3-labeled Goat Anti-Rat IgG (H+L) (1:300 dilution, A0507, Beyotime, Shanghai, China) for 1 hour at 37 °C under light-protected conditions. Nuclei were counterstained with 4′,6-diamidino-2-phenylindole (DAPI, C1005, Beyotime, Shanghai, China) for 10 minutes. Fluo-

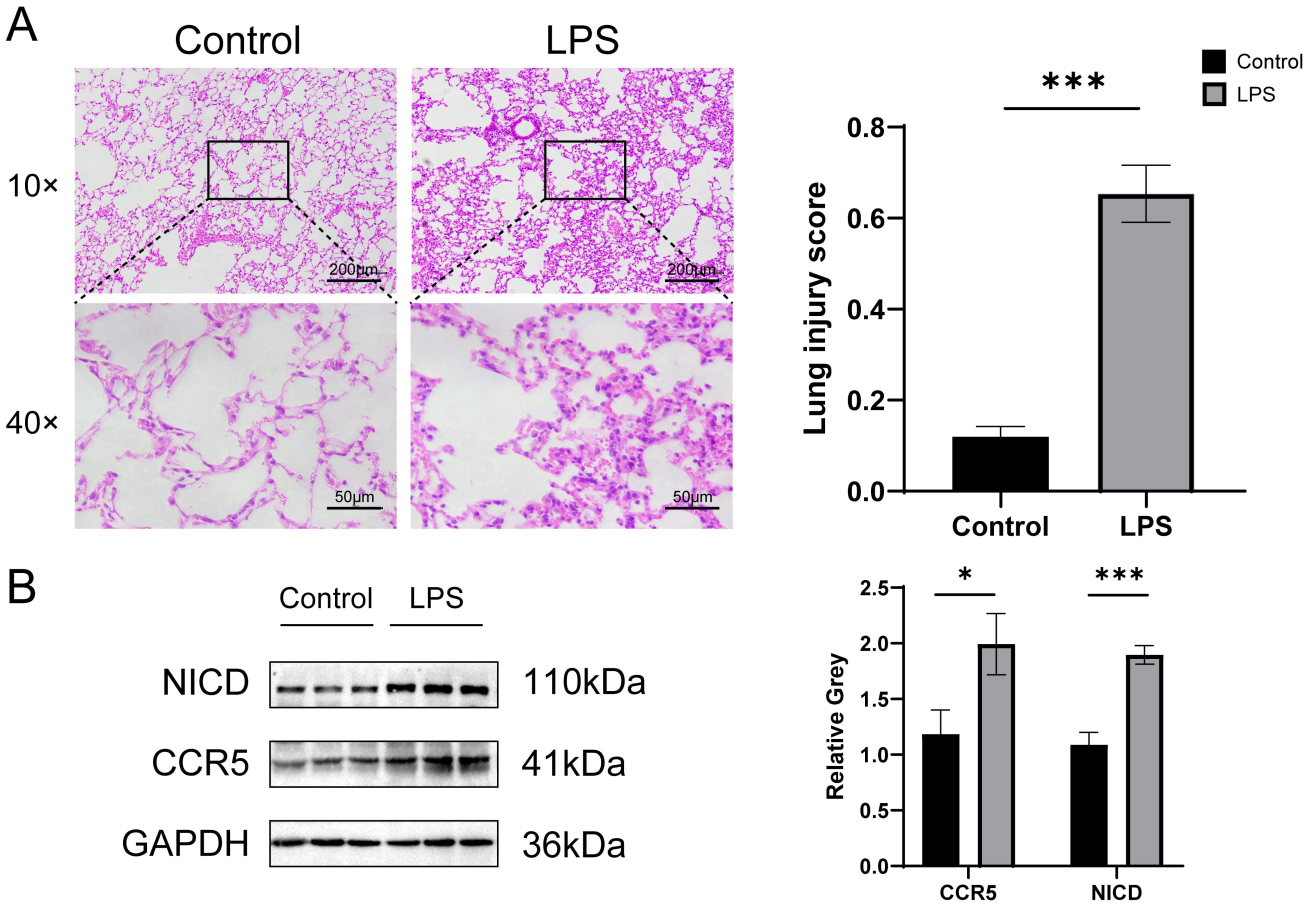

Fig. 1. Lung tissue pathology and protein expression in ALI mice. (A) hematoxylin and eosin (HE) staining of lung tissue sections and quantification of lung injury, n = 5. The magnification of the objective lens was 10× (Scale bar = 200 μm) and 40× (Scale bar = 50 μm), with an eyepiece magnification of 10×. (B) Western blot analysis of CCR5 and NICD levels in lung tissue and quantitative analysis, n = 3. *$p < 0.05$, ***$p < 0.001$. ALI, acute lung injury; NICD, Notch intracellular domain; LPS, lipopolysaccharide.

rescence imaging was conducted using an inverted fluorescence microscope (Olympus, Tokyo, Japan).

2.11 Wound Healing Assay

iBMDM cells were cultured in a 37 °C incubator until reaching 80% confluence. A sterile pipette tip was used to create a wound in the cell, and the cells were treated with 100 nM MK-0752 either in the presence or absence of LPS. The relative change in the scratch area over 12 hours was measured using ImageJ software to assess the effect of MK-0752 on LPS-induced cell migration. Images were captured at 0 hours, 6 hours, and 12 hours. The extent of cell migration was represented as the relative change in the scratch area compared to the 0-hour time point.

2.12 Transwell Migration Assay

iBMDM cells were seeded into the Transwell system and were divided into four groups: Control, LPS (1 μg/mL), LPS+CCL5 (10 ng/mL, P6780, Beyotime, Shanghai, China), and LPS+CCL5+MK-0752 (100 nM). A complete culture medium (600 μL) was added to the lower chamber, and 200 μL serum-free cell suspension with or without treatment was added to the upper chamber. LPS and MK-0752 were added to the upper chamber, while CCL5 was added to the lower chamber. After incubation at 37 °C for 12 hours, the unmigrated cells in the upper chamber were removed. The rest was stained with 0.1% crystal violet (C0121, Beyotime, Shanghai, China) for 20 minutes.

2.13 Statistical Analysis

All data were analyzed and processed using GraphPad Prism (version 10.0, GraphPad Software, LLC, San Diego, CA, USA) and were presented as the mean ± SD. Differences between the two groups were assessed using an unpaired *t*-test. Brown-Forsythe test was used to analyze whether the data complied with the homogeneity of variance. The Shapiro-Wilk test is used to verify the normal distribution. One-way ANOVA was used to compare groups before Tukey's post hoc test. The $p < 0.05$ was considered statistically significant.

3. Results

3.1 Lung Injury and CCR5 Expression in ALI Mice

To investigate the pathological mechanisms, initial analyses were conducted to evaluate pulmonary tissue alterations along with NICD and CCR5 expression levels in Notch1^{flox+} mice subjected to ALI. LPS stimulation destroys lung tissue architecture, which includes alveolar wall thickening, infiltration of red blood cells, and inflammatory cells in the alveoli and interstitium (Fig. 1A). Statistical evaluation demonstrated markedly elevated expression levels of CCR5 and NICD proteins in lung tissue homogenates obtained from LPS-treated animals relative to untreated control groups ($p < 0.05$, Fig. 1B). The experimental data indicate that LPS-triggered ALI activates the Notch pathway, and promotes protein expression of NICD, concomitant with enhanced CCR5 protein activity in pulmonary tissues.

3.2 Inhibition of CCR5 Alleviated Lung Lesion in ALI Mice

To investigate the therapeutic potential of CCR5 inhibition, mice were administered Maraviroc prior to LPS-induced ALI. Histopathological evaluation of pulmonary tissues demonstrated that Maraviroc pretreatment attenuated LPS-mediated lung injury, as evidenced by reduced alveolar septal thickening and inflammatory cell infiltration (Fig. 2A), accompanied by significantly lower histopathological scores (Fig. 2B, $p < 0.05$). Quantitative assessments revealed that Maraviroc administration significantly decreased pulmonary edema (wet-to-dry weight ratio), BALF cellularity, and total protein concentration compared to vehicle-treated controls (Fig. 2C–E, $p < 0.05$). Furthermore, pre-administration of Maraviroc markedly suppressed pulmonary expression of pro-inflammatory cytokines, including TNF-α, IL-6, and IL-1β, at the transcriptional level. Concurrently lessened their serum levels (Fig. 2F–K, $p < 0.05$). The successful establishment of the LPS-induced ALI model was confirmed by characteristic pathological features, including severe pulmonary damage, a significant increase in protein content in BALF, and elevated levels of proinflammatory cytokines in lung tissue. Inhibition of CCR5 alleviated lung tissue damage in ALI mice and reduced the expression of inflammatory cytokines.

3.3 Notch1 Mediated CCR5 Pro-inflammatory Effect

CCR5, as a receptor for inflammatory cell chemoattractants, is upregulated during the acute phase of ALI, potentially exacerbating secondary alveolar damage. It is therefore speculated that Notch may regulate CCR5 expression through ligand recognition, driving the accumulation of inflammatory cells and contributing to the pathological process.

To verify this hypothesis, we used macrophage Notch1 knockout mice to examine the effects of Notch1 deficiency on CCR5 activity in ALI. Analysis of BALF from ALI mice showed that both the total cell counts and total protein level in Notch1^{cre+} mice were significantly lower than those of Notch1^{flox+} mice ($p < 0.05$) (Fig. 3A,B). Flow cytometry analysis indicated that the percentage of CD45+CD64+ macrophages in lung tissue was comparable between Notch1^{cre+} and Notch1^{flox+} mice under baseline conditions. However, following LPS induction, the number of CD45+CD64+ cells in Notch1^{cre+} mice was significantly reduced compared to the Notch1^{flox+} control group ($p < 0.05$, Fig. 3C). Regarding CCR5 expression, no baseline differences were observed between Notch1^{flox+} and Notch1^{cre+} mice. Under physiological conditions, pulmonary NICD expression was markedly reduced in Notch1^{cre+} ($p < 0.05$, Fig. 3D). In the LPS-induced ALI model, both NICD and CCR5 protein levels in the lung tissue of Notch1^{cre+} and Notch1^{flox+} mice were increased, but the increase in Notch1^{cre+} mice was lower than in Notch1^{flox+} mice ($p < 0.05$, Fig. 3E). In different conditions, the transcriptional level of CCR5 in murine pulmonary tissue was correlated with its corresponding protein expression (Fig. 3F).

Immunofluorescence was used to detect CCR5 expression in alveolar macrophages, with anti-F4/80 (red) and anti-CCR5 (green) antibodies marking the macrophages to analyze CCR5 expression in macrophages of lung tissue. We found that under physiological conditions, the proportion of F4/80 and CCR5 double-positive cells in the lung tissue was low, with no significant difference between Notch1^{flox+} and Notch1^{cre+} mice ($p > 0.05$) (Fig. 3G). After LPS stimulation, F4/80 positivity increased in the lung tissues of both Notch1^{flox+} and Notch1^{cre+} mice, with higher fluorescence intensity observed in Notch1^{flox+} mice ($p < 0.05$, Fig. 3H). In contrast to Notch1^{flox+} mice, where CCR5 showed high expression after LPS stimulation, the expression of green fluorescent CCR5 was lower in the Notch1^{cre+} mice ($p < 0.05$, Fig. 3I). Furthermore, cells double-positive for F4/80 and CCR5 were scarcely observed in Notch1^{cre+} mice ($p < 0.05$, Fig. 3J).

The results indicate that although CCR5 expression in the lung tissue of Notch1^{cre+} mice increased after LPS stimulation, it was lower than that in Notch1^{flox+} mice. Additionally, the rare presence of F4/80 and CCR5 double-positive cells in Notch1^{cre+} mice suggests that Notch1 deficiency in alveolar macrophages impedes the expression of CCR5 on their cell membrane during LPS-induced ALI.

3.4 Inhibition of Notch Intracellular Signaling Reduces CCR5 Expression and Pro-inflammatory Cytokine Release in iBMDM Cells

To elucidate the regulatory role of the Notch signaling pathway on CCR5 expression under *in vitro* conditions, we employed MK-0752, a specific γ-secretase inhibitor, to suppress intracellular Notch signaling activity in iBMDM cells derived from murine sources. Following pharmaco-

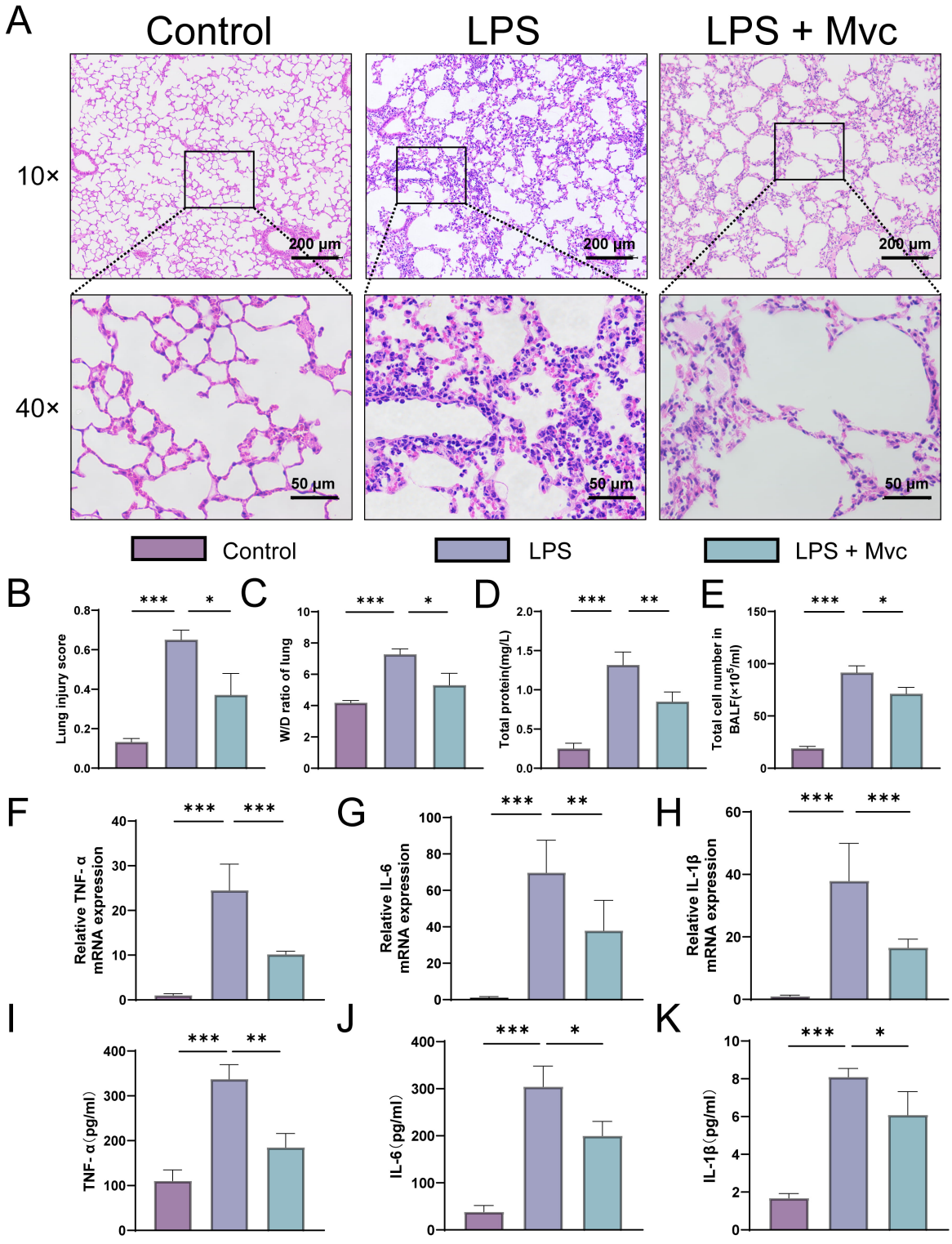

Fig. 2. CCR5 inhibition attenuated pulmonary damage in ALI. (A,B) Representative hematoxylin and eosin (H&E) lung sections and corresponding histopathological scoring n = 5; The magnification of the objective lens was 10× (Scale bar = 200 μm) and 40× (Scale bar = 50 μm). (C) Quantification of pulmonary edema through W/D weight ratio analysis n = 5. (D,E) Total cellularity and protein concentration in BALF n = 5. (F–H) qRT-PCR analysis of *TNF-α*, *IL-6*, and *IL-1β* mRNA levels in lung tissue, n = 5. (I–K) Enzyme-Linked Immunosorbent Assay (ELISA) detection of TNF-α, IL-6, and IL-1β levels in serum, n = 3. $*p < 0.05$, $**p < 0.01$, $***p < 0.001$. W/D, wet/dry; BALF, bronchoalveolar lavage fluid; qRT-PCR, real-time quantitative reverse transcription PCR; LPS+Mvc, LPS + Maraviroc.

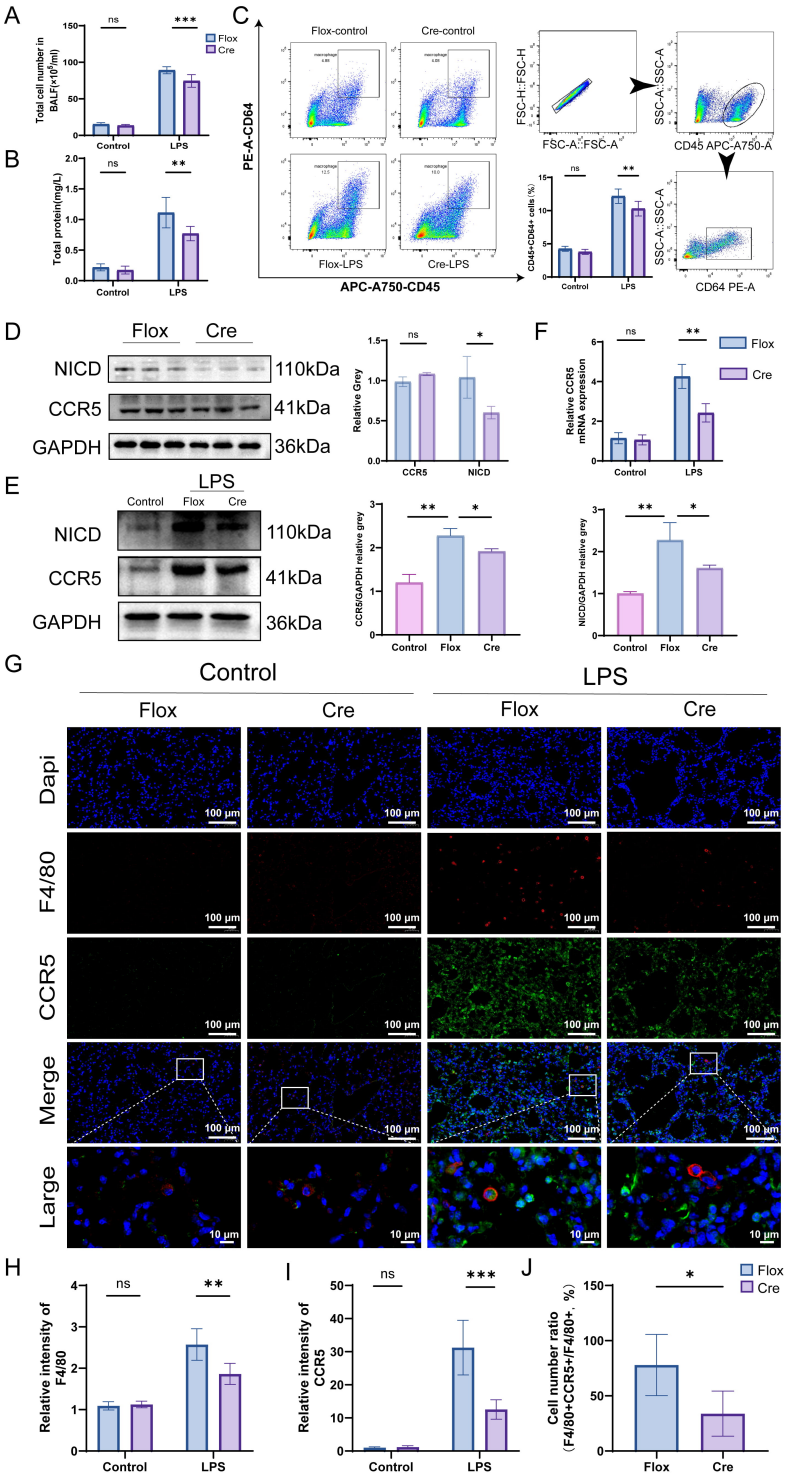

Fig. 3. Notch1-mediated CCR5 anti-inflammatory effect. (A,B) Total cell count and protein content in BALF, n = 5. (C) Flow cytometric analysis of lung tissue from mice and representative gating plots; Bar graphs represent the percentage of CD45+ and CD64+ macrophages of total cells. (D) Western blot analysis assessing NICD and CCR5 expression in lung tissue under normal conditions, n = 3. (E) Western blot analysis assessing NICD and CCR5 expression in lung tissue of wild-type and Notch1 knockout mice with LPS treatment, n = 3. (F) qRT-PCR detection of CCR5 mRNA levels in lung tissue of LPS-induced ALI mice, n = 5. (G) Immunofluorescence detection of CCR5 expression (green) in lung tissue macrophages (red). F4/80, red; CCR5, green; DAPI, blue; white box in each image indicates magnified views in the inset; magnification 40×, scale bar = 100 μm. The scale bar in the large image is 10 μm. (H,I) Quantification of F4/80 and CCR5 fluorescence intensity. (J) Percentage of F4/80 and CCR5 double-positive cells among F4/80-positive cells, n = 5. *$p < 0.05$, **$p < 0.01$, ***$p < 0.001$, ns indicates no statistical significance. DAPI, 4′,6-diamidino-2-phenylindole.

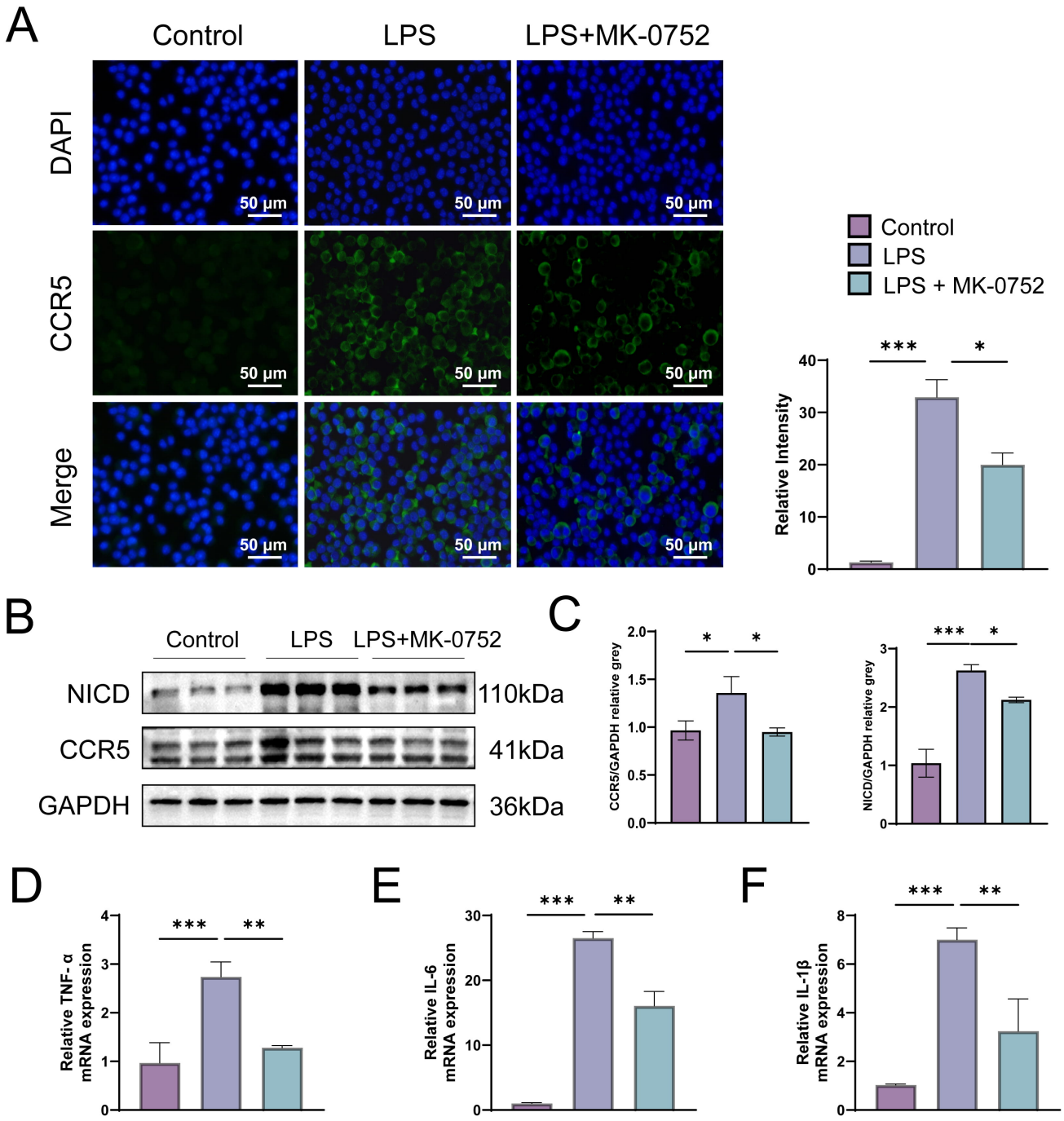

Fig. 4. Inhibition of the Notch pathway reduces CCR5 transcription and pro-inflammatory cytokine expression in LPS-induced iBMDM cells. (A) Immunofluorescence was used to detect CCR5 expression (green) on iBMDM cells, with DAPI staining (blue) for nuclei. The fluorescence intensity was quantified. Magnification: 40×, scale bar = 50 μm. (B,C) Western blot analysis was used to assess NICD and CCR5 protein levels in iBMDM cells under different treatments, with quantitative analysis of the protein expression. (D–F) qRT-PCR was used to detect the mRNA levels of *TNF-α*, *IL-6*, and *IL-1β* in LPS-induced iBMDM cells, n = 3. *$p < 0.05$, **$p < 0.01$, ***$p < 0.001$. iBMDM, immortalized bone marrow-derived macrophages.

logical inhibition, the protein expression levels of CCR5 were quantitatively assessed in the treated iBMDM cellular model.

As illustrated in Fig. 4A, LPS stimulation markedly enhanced CCR5 fluorescence intensity on the cellular membrane, a phenomenon that was substantially inhibited by MK-0752 administration. Consistent with these findings, western blot analysis demonstrated a concomitant increase in both CCR5 and NICD protein levels upon LPS challenge, which were prominently downregulated in iBMDM

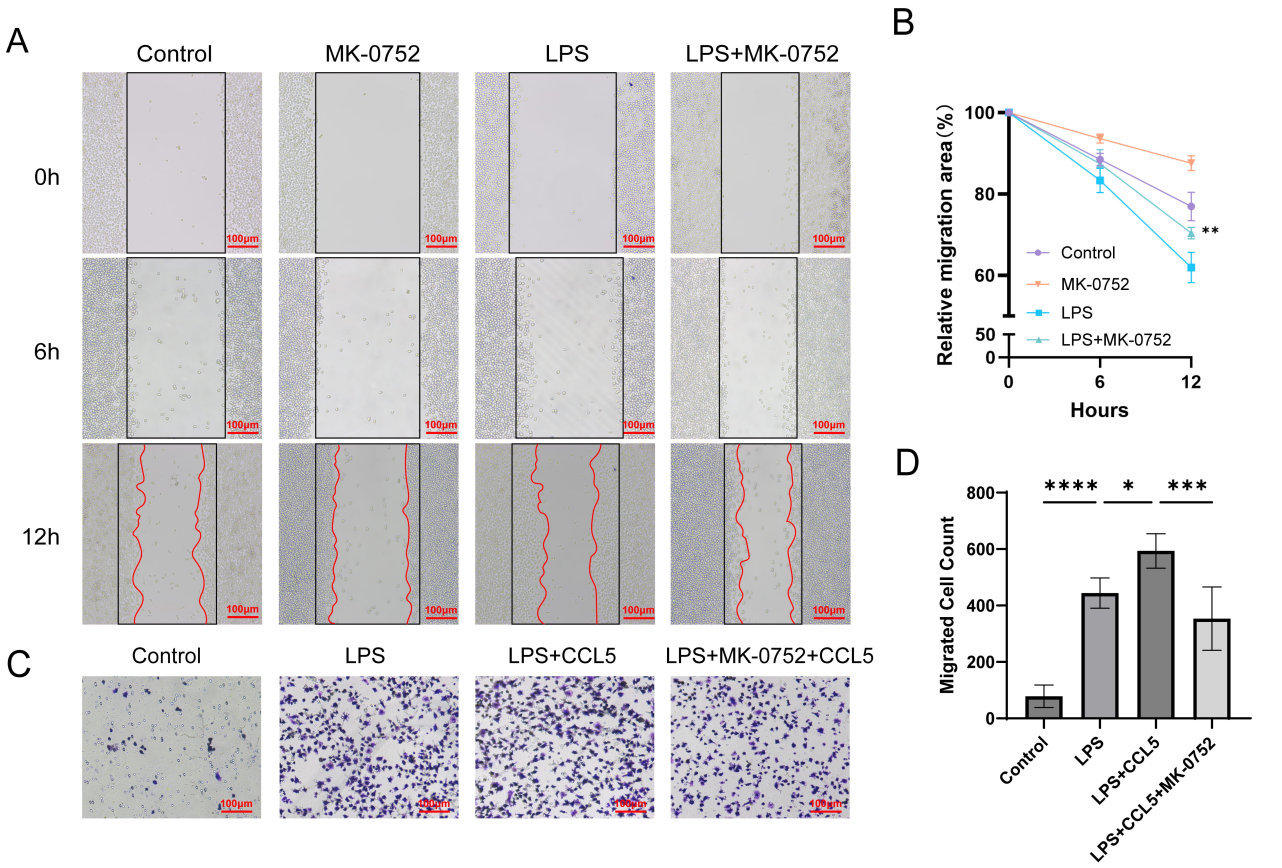

Fig. 5. Inhibition of the Notch pathway reduces the migration efficiency of iBMDM cells. (A) Migration of iBMDM cells under Notch inhibition was assessed using the wound healing assay. (B) Quantification of the migration rate of iBMDM cells at 6 and 12 hours. LPS group VS LPS+MK-0752 group $^{**}p < 0.01$. (C) Migration of iBMDM cells was observed through crystal violet staining. (D) Quantitative analysis of the number of migrated iBMDM cells in each group, n = 3, magnification: 10×, scale bar = 100 μm. $^{*}p < 0.05$, $^{***}p < 0.001$, $^{****}p < 0.0001$.

cells pretreated with MK-0752 prior to LPS exposure ($p < 0.05$) (Fig. 4B,C). Furthermore, quantitative PCR analysis revealed that pharmacological blockade of γ-secretase activity significantly suppressed LPS-induced transcriptional upregulation of IL-6, IL-1β, and TNF-α ($p < 0.05$), as evidenced in Fig. 4D–F. These findings indicate that the intracellular Notch signaling in macrophages is closely linked to CCR5 expression and the transcription of pro-inflammatory cytokines, which was dependent on the activity of γ-secretase.

3.5 Notch Pathway Mediates Macrophage Migration Efficiency through CCR5

The activation of Notch receptors on macrophages, upon binding with ligands from neighboring cells, triggers the release of chemokines that orchestrate the recruitment and migration of immune cells to the lungs, thereby exacerbating lung injury [15]. CCR5, as a chemokine receptor, plays an important role in regulating macrophage migration [16,17]. Therefore, we investigated whether Notch signaling affects macrophage migration through CCR5 expression. Since primary macrophages *in vitro* are adherent and difficult to track for migration efficiency, this part of the experiment utilized LPS-induced iBMDM cell migration for analysis.

The wound healing assay showed that under MK-0752-mediated γ-secretase inhibition, LPS-induced migration of iBMDM cells was also suppressed (Fig. 5A,B). We further used the Transwell assay to verify whether this migratory inhibition occurs through the CCR5 pathway. After LPS stimulation, the migration of iBMDM cells treated with CCL5 significantly increased. However, under γ-secretase inhibition by MK-0752, the ability of CCL5 to recruit cells was notably reduced (Fig. 5C,D). These experimental findings provide additional evidence that Notch signaling activation in macrophages potentially mediates the CCL5-induced macrophage aggregation by modulating CCR5 activity.

4. Discussion

Sepsis is one of the leading causes of ALI and ARDS, which can progress rapidly, even resulting in death in severe cases. This investigation provides evidence that NICD and

CCR5 expression undergo significant upregulation within pulmonary tissues during ALI in a murine model. In addition, the pharmacological blockade of CCR5 signaling demonstrates therapeutic potential in mitigating LPS-induced pulmonary tissue pathology, indicating a crucial involvement of CCR5 in the molecular mechanisms underlying ALI pathogenesis. The absence of Notch1 signaling or inhibition of the intracellular domain significantly reduces CCR5 expression in ALI lung macrophages, alleviates lung tissue damage, and weakens macrophage recruitment and migration mediated by CCR5. This study provides a theoretical foundation for immune modulation therapies targeting the Notch pathway.

The proliferation, differentiation, and functional activation of myeloid and lymphocyte populations are widely regulated by the Notch signaling cascade [18]. The Notch receptor family consists of four subtypes (Notch1-4), which are activated upon binding to external ligands (Delta/Jagged). This proteolytic activation results in γ-secretase-mediated cleavage of the NICD [19]. Notch signaling on macrophages can play its biological role by cascading with NF-κB signaling to drive transcriptional activation of key pro-inflammatory mediators such as TNF-α [20]. Additionally, disruption of Notch signaling cascades results in the downregulation of multiple pro-inflammatory cytokine networks, suggesting its critical role in modulating macrophage-mediated inflammatory responses [21,22]. We observed that LPS stimulation activates Notch signaling in mouse lung tissue, with increased expression of the intracellular NICD. Both Notch deficiency and the blockade of intracellular signaling reduce the transcription of cytokines in macrophages. The Notch signaling cascade serves as a crucial regulatory mechanism governing macrophage migratory dynamics, with research demonstrating that the activation of Notch signaling through the Jagged1 ligand facilitates the metastatic progression of malignant tumors [23]. There are few reports on the regulation of macrophage migration through the Notch signaling pathway under inflammatory conditions. In this study, based on the ALI model constructed in macrophage Notch1 knockout mice, we found that Notch1 knockout alleviates pulmonary edema, alveolar hemorrhage, protein leakage, and macrophage infiltration in the lungs.

The directed migration of macrophages to the damaged areas is a key factor driving acute lung injury and exacerbating the inflammatory response. LPS can activate macrophages and polarize them into the M1 phenotype, producing pro-inflammatory cytokines such as RANTES (CCL5) [24,25], which recruit more inflammatory cells to the affected lung, thereby intensifying the inflammatory response in ALI. A previous study has suggested that monocyte accumulation in lung injury is mediated by CCR2 [26]. Nevertheless, accumulating experimental data suggest that CCR5 contributes significantly to this biological mechanism. In sepsis models, monocytes with high CCR5 expression show increased migration into the circulatory system, contributing to disease progression [27]. Moreover, the activation of CCR5 is not limited to promoting the migration of immune cells; it also affects their activation state and function, thereby controlling the release of inflammatory mediators. The chemokine CCL5 mediates activation of both MAPK and NF-κB signaling cascades via CCR5 receptor engagement, thereby inducing macrophage polarization into the M1 subtype and subsequently amplifying tissue injury [28]. Our experimental data demonstrated upregulated CCR5 expression in pulmonary tissues of ALI models. Pharmacological inhibition of CCR5 significantly ameliorated histopathological alterations, attenuated inflammatory cell recruitment, and suppressed pro-inflammatory mediator secretion, corroborating existing literature reports [11,29]. These findings demonstrate that controlling inflammation via the CCR5 pathway could serve as a potential protective strategy for ALI.

The recombination signal binding protein for immunoglobulin kappa J region (RBP-Jκ) serves as a central downstream component of the Notch signaling. Following NICD binding, RBP-Jκ undergoes a molecular transition from transcriptional repression to activation state, thereby driving the activation of downstream target genes [30]. A recent study has identified a functional cooperation between RBP-Jκ and Transforming Growth Factor-beta 1 (TGF-β1) TGF-β1/ Suppressor of Mothers Against Decapentaplegic homolog 3 (Smad3) signaling pathway in Th9 cell differentiation, where these molecular components work in concert to transcriptionally activate IL-9 gene expression. [31]. In addition, in the context of HIV-1 infection, TGF-β1 enhances the activation and expression of CCR5 on resting memory CD4$^+$ T cells through a Smad3-dependent mechanism, facilitating viral entry and immune evasion [32]. These experimental observations collectively underscore the critical involvement of the RBP-Jκ/TGF-β1/Smad3 signaling axis in multiple pathological processes, ranging from cancer metastasis to viral pathogenesis. These findings provide mechanistic evidence that Notch signaling is functionally linked to CCR5 expression, potentially through direct transcriptional regulation or downstream signaling cascades. A previous study has demonstrated that in mammary carcinoma pathogenesis, lactate can activate the Notch signaling in macrophages, thereby controlling cancer cell migration through the CCL5-CCR5 axis [33]. Our results show that in the absence of Notch1 or when intracellular signaling is inhibited, CCR5 expression levels in pulmonary tissues and macrophage counts in BALF demonstrated significant reduction. *In vitro* experimental data demonstrated that pharmacological blockade of Notch signaling significantly attenuated macrophage migratory capacity, and even after exogenous CCL5 stimulation, this trend could not be fully reversed. This suggests that inhibition of the Notch pathway reduces CCR5 activity, affecting the CCL5/CCR5 axis, which in turn diminishes

macrophage migration and decreases inflammatory mediator release. Our results confirm that the protective effect of Notch1 signal inhibition in ALI mice may be achieved by lowering the expression of CCR5 on macrophage membranes, thereby inhibiting cell migration, infiltration, and the release of inflammatory mediators.

Undeniably, there are some limitations in our research. To be specific, we only validated the role of Notch and CCR5 in macrophages. Nevertheless, the pathogenesis of acute inflammatory responses involves complex interactions among multiple immune cell populations and cytokine networks through diverse signaling cascades. Further studies are needed to complement and expand on these findings. Additionally, our study is based solely on animal and cell models, lacking corresponding clinical data. Further comprehensive investigations are warranted to elucidate the interplay between Notch signaling and CCR5 pathways in ALI pathogenesis, which may facilitate the development of novel therapeutic strategies for clinical translation.

5. Conclusion

Collectively, our experimental findings demonstrate that Notch signaling pathway modulation attenuates LPS-induced ALI progression through CCR5-mediated mechanisms, leading to reduced macrophage infiltration and inflammatory cascade activation. These findings identify the Notch-CCR5 signaling axis as a potential therapeutic target for the treatment of ALI.

Availability of Data and Materials

The original contributions made in this study have been incorporated into the article and **Supplementary Materials**. For any further inquiries, please direct them to the corresponding author.

Author Contributions

RYZ and DCZ conceptualized the study design. HD, YXL, HZH, JWZ, PY and DCZ wrote the initial drafts of the manuscript. All authors read and approved the final report and have no conflicting issues with the contributions listed herein. RYZ, HD: Designed the experiments; Performed the experiments; Collected and analyzed data; Wrote the paper. ZL, YXL, HZH, JWZ: Participated in experiments; Made figures; Provided technical support. PY, DCZ: Designed the experiments, Supervision, and Funding acquisition. All authors approved the final version of this manuscript. All authors contributed to editorial changes in the manuscript. All authors have participated sufficiently in the work and agreed to be accountable for all aspects of the work.

Ethics Approval and Consent to Participate

This study was approved by The Animal Ethics Committee of Wuhan University (NO. WP20240088), adhered to the Animal Research: Reporting of *In Vivo* Experiments (ARRIVE) guidelines 2019.

Acknowledgment

Not applicable.

Funding

This study was funded by the National Natural Science Foundation of China (81670007).

Conflict of Interest

The authors declare no conflict of interest.

Supplementary Material

Supplementary material associated with this article can be found, in the online version, at https://doi.org/10.31083/FBL37430.

References

[1] ARDS Definition Task Force, Ranieri VM, Rubenfeld GD, Thompson BT, Ferguson ND, Caldwell E, *et al*. Acute respiratory distress syndrome: the Berlin Definition. JAMA. 2012; 307: 2526–2533. https://doi.org/10.1001/jama.2012.5669.

[2] Mokrá D. Acute lung injury - from pathophysiology to treatment. Physiological Research. 2020; 69: S353–S366. https://doi.org/10.33549/physiolres.934602.

[3] Byrne AJ, Mathie SA, Gregory LG, Lloyd CM. Pulmonary macrophages: key players in the innate defence of the airways. Thorax. 2015; 70: 1189–1196. https://doi.org/10.1136/thoraxjnl-2015-207020.

[4] Yang Y, Ni M, Zong R, Yu M, Sun Y, Li J, *et al*. Targeting Notch1-YAP Circuit Reprograms Macrophage Polarization and Alleviates Acute Liver Injury in Mice. Cellular and Molecular Gastroenterology and Hepatology. 2023; 15: 1085–1104. https://doi.org/10.1016/j.jcmgh.2023.01.002.

[5] Song J, Peng D, Peng Y, Zhao G, Ren Y, Guo L, *et al*. The new pattern for dual NOTCH pathway involving nuclear transcription and mitochondrial regulation supports therapeutic mechanism of 4-butyl benzophenone derivatives against SIRS. Free Radical Biology & Medicine. 2024; 223: 306–324. https://doi.org/10.1016/j.freeradbiomed.2024.07.036.

[6] Clua P, Tomokiyo M, Raya Tonetti F, Islam MA, García Castillo V, Marcial G, *et al*. The Role of Alveolar Macrophages in the Improved Protection against Respiratory Syncytial Virus and Pneumococcal Superinfection Induced by the Peptidoglycan of *Lactobacillus rhamnosus* CRL1505. Cells. 2020; 9: 1653. https://doi.org/10.3390/cells9071653.

[7] Zeng Z, Lan T, Wei Y, Wei X. CCL5/CCR5 axis in human diseases and related treatments. Genes & Diseases. 2022; 9: 12–27. https://doi.org/10.1016/j.gendis.2021.08.004.

[8] Holloman BL, Cannon A, Wilson K, Singh N, Nagarkatti M, Nagarkatti P. Characterization of Chemotaxis-Associated Gene Dysregulation in Myeloid Cell Populations in the Lungs during Lipopolysaccharide-Mediated Acute Lung Injury. Journal of Immunology (Baltimore, Md.: 1950). 2023; 210: 2016–2028. https://doi.org/10.4049/jimmunol.2200822.

[9] Ravi AK, Khurana S, Lemon J, Plumb J, Booth G, Healy L, *et al*. Increased levels of soluble interleukin-6 receptor and CCL3 in COPD sputum. Respiratory Research. 2014; 15: 103. https://doi.org/10.1186/s12931-014-0103-4.

[10] Chua RL, Lukassen S, Trump S, Hennig BP, Wendisch D, Pott

F, *et al*. COVID-19 severity correlates with airway epithelium-immune cell interactions identified by single-cell analysis. Nature Biotechnology. 2020; 38: 970–979. https://doi.org/10.1038/s41587-020-0602-4.

[11] Chernov AS, Rodionov MV, Kazakov VA, Ivanova KA, Meshcheryakov FA, Kudriaeva AA, *et al*. CCR5/CXCR3 antagonist TAK-779 prevents diffuse alveolar damage of the lung in the murine model of the acute respiratory distress syndrome. Frontiers in Pharmacology. 2024; 15: 1351655. https://doi.org/10.3389/fphar.2024.1351655.

[12] Alghibiwi H, Ansari MA, Nadeem A, Algonaiah MA, Attia SM, Bakheet SA, *et al*. DAPTA, a C-C Chemokine Receptor 5 (CCR5), Leads to the Downregulation of Notch/NF-κB Signaling and Proinflammatory Mediators in $CD40^+$ Cells in Experimental Autoimmune Encephalomyelitis Model in SJL/J Mice. Biomedicines. 2023; 11: 1511. https://doi.org/10.3390/biomedicines11061511.

[13] Dhlamini Q, Wang W, Feng G, Chen A, Chong L, Li X, *et al*. FGF1 alleviates LPS-induced acute lung injury via suppression of inflammation and oxidative stress. Molecular Medicine (Cambridge, Mass.). 2022; 28: 73. https://doi.org/10.1186/s10020-022-00502-8.

[14] Matute-Bello G, Downey G, Moore BB, Groshong SD, Matthay MA, Slutsky AS, *et al*. An official American Thoracic Society workshop report: features and measurements of experimental acute lung injury in animals. American Journal of Respiratory Cell and Molecular Biology. 2011; 44: 725–738. https://doi.org/10.1165/rcmb.2009-0210ST.

[15] Wang J, Peng X, Yuan N, Wang B, Chen S, Wang B, *et al*. Interplay between pulmonary epithelial stem cells and innate immune cells contribute to the repair and regeneration of ALI/ARDS. Translational Research: the Journal of Laboratory and Clinical Medicine. 2024; 272: 111–125. https://doi.org/10.1016/j.trsl.2024.05.012.

[16] van Elsas MJ, Middelburg J, Labrie C, Roelands J, Schaap G, Sluijter M, *et al*. Immunotherapy-activated T cells recruit and skew late-stage activated M1-like macrophages that are critical for therapeutic efficacy. Cancer Cell. 2024; 42: 1032–1050.e10. https://doi.org/10.1016/j.ccell.2024.04.011.

[17] Zoshima T, Baba T, Tanabe Y, Ishida Y, Nakatani K, Nagata M, *et al*. CCR2- and CCR5-mediated macrophage infiltration contributes to glomerular endocapillary hypercellularity in antibody-induced lupus nephritis. Rheumatology (Oxford, England). 2022; 61: 3033–3048. https://doi.org/10.1093/rheumatology/keab825.

[18] Radtke F, Fasnacht N, Macdonald HR. Notch signaling in the immune system. Immunity. 2010; 32: 14–27. https://doi.org/10.1016/j.immuni.2010.01.004.

[19] Zhao K, Chen L, Xie Y, Ren N, Li J, Zhai X, *et al*. m6A/HOXA10-AS/ITGA6 axis aggravates oxidative resistance and malignant progression of laryngeal squamous cell carcinoma through regulating Notch and Keap1/Nrf2 pathways. Cancer Letters. 2024; 587: 216735. https://doi.org/10.1016/j.canlet.2024.216735.

[20] Monsalve E, Ruiz-García A, Baladrón V, Ruiz-Hidalgo MJ, Sánchez-Solana B, Rivero S, *et al*. Notch1 upregulates LPS-induced macrophage activation by increasing NF-kappaB activity. European Journal of Immunology. 2009; 39: 2556–2570. https://doi.org/10.1002/eji.200838722.

[21] Hu X, Chung AY, Wu I, Foldi J, Chen J, Ji JD, *et al*. Integrated regulation of Toll-like receptor responses by Notch and interferon-gamma pathways. Immunity. 2008; 29: 691–703. https://doi.org/10.1016/j.immuni.2008.08.016.

[22] Tsao PN, Wei SC, Huang MT, Lee MC, Chou HC, Chen CY, *et al*. Lipopolysaccharide-induced Notch signaling activation through JNK-dependent pathway regulates inflammatory response. Journal of Biomedical Science. 2011; 18: 56. https://doi.org/10.1186/1423-0127-18-56.

[23] Tao S, Chen Q, Lin C, Dong H. Linc00514 promotes breast cancer metastasis and M2 polarization of tumor-associated macrophages via Jagged1-mediated notch signaling pathway. Journal of Experimental & Clinical Cancer Research: CR. 2020; 39: 191. https://doi.org/10.1186/s13046-020-01676-x.

[24] Wu B, Xu MM, Fan C, Feng CL, Lu QK, Lu HM, *et al*. STING inhibitor ameliorates LPS-induced ALI by preventing vascular endothelial cells-mediated immune cells chemotaxis and adhesion. Acta Pharmacologica Sinica. 2022; 43: 2055–2066. https://doi.org/10.1038/s41401-021-00813-2.

[25] Jiang W, Zhang Y, Sheng Y, Liu M, Du C, Pan X, *et al*. Overexpression of IFIT1 protects against LPS-induced acute lung injury via regulating CCL5-p65NF-κB signaling. International Immunopharmacology. 2023; 114: 109485. https://doi.org/10.1016/j.intimp.2022.109485.

[26] Coates BM, Staricha KL, Koch CM, Cheng Y, Shumaker DK, Budinger GRS, *et al*. Inflammatory Monocytes Drive Influenza A Virus-Mediated Lung Injury in Juvenile Mice. Journal of Immunology (Baltimore, Md.: 1950). 2018; 200: 2391–2404. https://doi.org/10.4049/jimmunol.1701543.

[27] Castanheira FVES, de Lima KA, Cebinelli GCM, Sônego F, Kanashiro A, Colon DF, *et al*. CCR5-Positive Inflammatory Monocytes are Crucial for Control of Sepsis. Shock (Augusta, Ga.). 2019; 52: e100–e106. https://doi.org/10.1097/SHK.0000000000001301.

[28] Li M, Sun X, Zhao J, Xia L, Li J, Xu M, *et al*. CCL5 deficiency promotes liver repair by improving inflammation resolution and liver regeneration through M2 macrophage polarization. Cellular & Molecular Immunology. 2020; 17: 753–764. https://doi.org/10.1038/s41423-019-0279-0.

[29] Grommes J, Drechsler M, Soehnlein O. CCR5 and FPR1 mediate neutrophil recruitment in endotoxin-induced lung injury. Journal of Innate Immunity. 2014; 6: 111–116. https://doi.org/10.1159/000353229.

[30] Morrow D, Guha S, Sweeney C, Birney Y, Walshe T, O'Brien C, *et al*. Notch and vascular smooth muscle cell phenotype. Circulation Research. 2008; 103: 1370–1382. https://doi.org/10.1161/CIRCRESAHA.108.187534.

[31] Elyaman W, Bassil R, Bradshaw EM, Orent W, Lahoud Y, Zhu B, *et al*. Notch receptors and Smad3 signaling cooperate in the induction of interleukin-9-producing T cells. Immunity. 2012; 36: 623–634. https://doi.org/10.1016/j.immuni.2012.01.020.

[32] Yim LY, Lam KS, Luk TY, Mo Y, Lu X, Wang J, *et al*. Transforming Growth Factor β Signaling Promotes HIV-1 Infection in Activated and Resting Memory $CD4^+$ T Cells. Journal of Virology. 2023; 97: e0027023. https://doi.org/10.1128/jvi.00270-23.

[33] Lin S, Sun L, Lyu X, Ai X, Du D, Su N, *et al*. Lactate-activated macrophages induced aerobic glycolysis and epithelial-mesenchymal transition in breast cancer by regulation of CCL5-CCR5 axis: a positive metabolic feedback loop. Oncotarget. 2017; 8: 110426–110443. https://doi.org/10.18632/oncotarget.22786.